Molecular Therapy
Nucleic Acids
Original Article

Membrane tethering of CreER decreases uninduced cell labeling and cytotoxicity while maintaining recombination efficiency

Mianqiao Chen,[1] Xiong Tian,[1] Liqun Xu,[1] Ruolan Wu,[1] Haoming He,[1] Haibao Zhu,[1] Wencan Xu,[3] and Chi-ju Wei[1,2]

[1]Guangdong Provincial Key Laboratory of Marine Biotechnology, Institute of Marine Sciences, Shantou University, Shantou, Guangdong 515063, China; [2]Multidisciplinary Research Center, Shantou University, Shantou, Guangdong 515063, China; [3]Department of Endocrinology, the First Affiliated Hospital of Shantou University Medical College, Shantou, Guangdong 515041, China

Genetic lineage tracing is indispensable to unraveling the origin, fate, and plasticity of cells. However, the intrinsic leakiness in the CreER-*loxP* system raises concerns on data interpretation. Here, we reported the generation of a novel dual inducible CreER-*loxP* system with superior labeling characteristics. This two-component system consists of membrane localized CreER (mCreER: CD8α-FRB-CS-CreER) and TEV protease (mTEVp: CD8α-FKBP-TEVp), which are fusion proteins incorporated with the chemically induced dimerization machinery. Rapamycin and tamoxifen induce sequential dimerization of FKBP and FRB, cleavage of CreER from the membrane, and translocation into the nucleus. The labeling leakiness in Ad293 cells reduced dramatically from more than 70% to less than 5%. This tight labeling feature depends largely on the association of mCreER with HSP90, which conceals the TEV protease cutting site between FRB and CreER and thus preventing uninduced cleavage of the membrane-tethering CreER. Membrane-bound CreER also diminished significantly cytotoxicity. Our studies showed mCreER under the control of the rat insulin promoter increased labeling specificity in MIN6 islet beta-cells. Viability and insulin secretion of MIN6 cells remained intact. Our results demonstrate that this novel system can provide more stringent temporal and spatial control of gene expression and will be useful in cell fate probing.

INTRODUCTION

Lineage tracing is a powerful tool for unraveling the origin, fate, and plasticity of cells in tissue regeneration, homeostasis, and disease progression in the context of an intact tissue or organism.[1,2] Lineage tracing is also indispensable to providing spatial, temporal, and kinetic resolution at the single-cell level of the mechanisms that underlie tissue remodeling under physical and pathological conditions.[3,4] The Cre-*loxP* recombination system, including the tamoxifen-inducible CreER-*loxP*,[5] is the most widely used technology for *in vivo* stem cell and progenitor cell tracing. Since its development in the 1980s,[6,7] this versatile system has found applications in virtually almost every genetically engineered organism and has greatly expanded our ability to precisely interrogate gene function, cell behavior, and treatment of diseases.[8–10]

Awareness and concerns, however, on the limitations and caveats of the Cre-*loxP* technology have been raised repeatedly.[11,12] Numerous studies have demonstrated that the CreER-*loxP* system exhibits leakiness to an extent, which means the occurrence of spontaneous cell labeling in the absence of tamoxifen induction (Table S4). For example, Kemp et al.[13] reported sporadic recombination at the R26R reporter locus in multiple tissues of mice carrying a CreER transgene under the control of a constitutively active promoter. Similarly, Kristianto et al.[14] found 10%–80% unintended Cre activities in all examined tissues of mice from crossing a CreER driver line with two reporter strains, raising the possibility of this confounding background activity might impact largely on data interpretation. The famous rat insulin promoter (RIP) has been used extensively to probe gene function specifically in pancreatic islet beta-cells. However, mice with a transgenic Cre under the control of RIP display glucose intolerance in the absence of genes targeted by *loxP* sites.[15] Apparently, the expression of Cre alone in beta-cells could lead to the cleavage of cryptic *loxP* sites in the genome and thus compromise insulin secretion.[16] Further, Liu et al.[17] have reported the detection of tamoxifen-independent Cre activity as early as 2 months of age in RIP-CreER mice crossed with three distinct reporter strains. Leakiness in various degrees also exists in other transgenic mice carrying a tissue specifically expressed CreER gene, such as Gcg-CreER, Opn-CreER, Ck19-CreER, and Col2a1-CreER.[18–20]

A plethora of distinctive and even contradictory observations have been reported regarding the mechanisms of beta-cell development in adult mice by using the Cre-*loxP* technology. Dor et al.[21] found replication of preexisting beta-cells, instead of neogenesis from islet

Received 17 May 2021; accepted 28 January 2022;
https://doi.org/10.1016/j.omtn.2022.01.022.

Correspondence: Chi-ju Wei, PhD, Guangdong Provincial Key Laboratory of Marine Biotechnology, Institute of Marine Sciences, Shantou University, Shantou, Guangdong 515063, China.
E-mail: chijuwei@stu.edu.cn

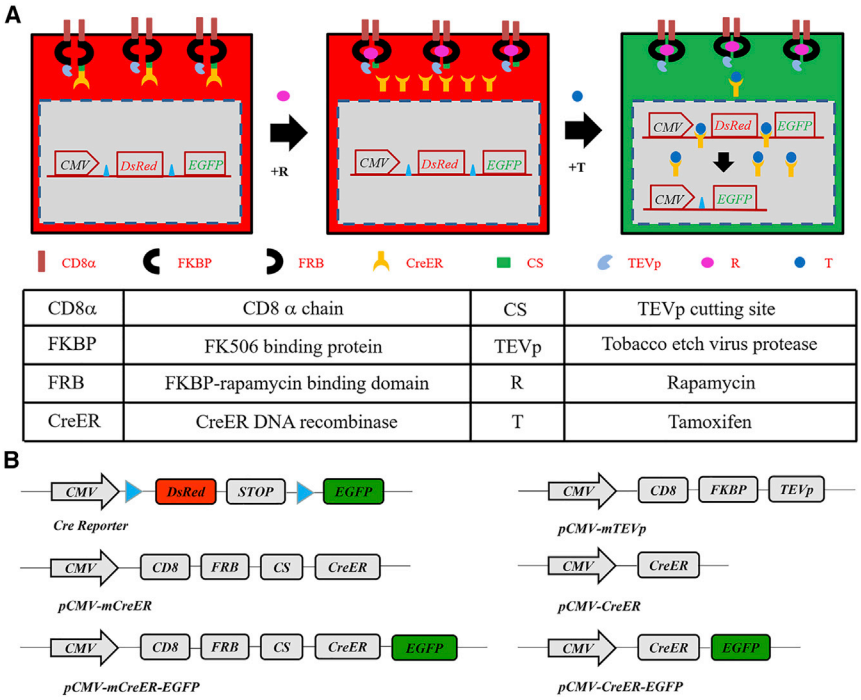

CD8α	CD8 α chain	CS	TEVp cutting site
FKBP	FK506 binding protein	TEVp	Tobacco etch virus protease
FRB	FKBP-rapamycin binding domain	R	Rapamycin
CreER	CreER DNA recombinase	T	Tamoxifen

Figure 1. Construction of a dual inducible CreER cell labeling system

(A) Schematic diagram and labeling mechanism. (B) Schematic diagram of plasmids used in this study. Blue triangles: *loxP* sites.

progenitor cells, is the major cause responsible for beta-cell homeostasis in mice under normal physiology or partial pancreatectomy. Subsequent studies by Nir et al.[22] and Teta et al.[23] concluded that there is little or no progenitor cell activity in the adult pancreas. However, evidence supporting the existence of islet progenitors is also overwhelming.[24,25] By using the same cell tracing technology, Inada et al.[26] showed that carbonic anhydrase II-positive pancreatic ductal cells could serve as facultative progenitors that gave rise to both new islets and acini in neonates and duct-ligated mice. Recently, Wang et al.[27] describe a previously unidentified protein C receptor positive (Procr^{+}) progenitor cell population in adult mouse pancreas, which can undergo clonal expansion and generate all four endocrine cell types during adult homeostasis. Likewise, the existence of stem cells in some other tissues, such as cardiac muscle stem cells and cancer stem cells, is also heatedly debated.[28,29]

In this study, we presented a dual inducible membrane-localized CreER-*loxP* system, which displays superior labeling capacity and low cytotoxicity. The system could be invaluable to cell lineage tracing and resolving the controversy surrounding the existence of stem cells in multiple adult tissues.

RESULTS

The dual inducible CreER-*loxP* system increases cell labeling stringency

This bipartite system is composed of a membrane-localized CreER (mCreER) and a membrane-bound TEV protease (mTEVp) (Figure 1A). CreER was targeted to the plasma membrane by fusion C-terminally to the CD8α chain, while an FRB fragment containing a TEV protease cutting site (CS) was inserted in between. Membrane-bound TEV protease was created similarly by fusion with CD8α and FKBP. Induction with rapamycin stimulated dimerization between FKBP and FRB, leading to cleavage at CS by TEVp and releasing of CreER from the membrane. Addition of tamoxifen stimulates nucleus translocation of CreER, resulting in recombination between two *loxP* sites. Deletion of the dsRed fragment in the Cre reporter construct (*pCMV-loxP-DsRed-STOP-loxP-EGFP*, STOP: a poly-A signal for transcriptional termination) puts the EGFP gene under the control of the CMV promoter (Figure 1A).

To test the above hypothesis, we generated a series of CreER constructs (Figures 1B and S1). The classical CreER-*loxP* system consists of the Cre reporter and *pCMV-CreER*, which produces a cytoplasm-localized CreER. The dual inducible CreER cell labeling system consists of the *pCMV-mCreER* and *pCMV-mTEVp*, which produce both membrane-tethered CreER and TEVp. For the detection of the cellular localization of CreER, we generated *pCMV-mCerER-EGFP* and *pCMV-CreER-EGFP*. To evaluate the effect of the relative position between CS and ER, we generated *pCMV-CD8-FRB-CS-ER-Cre*, *pCMV-CD8-FRB-ER-Cre-EGFP*, *pCMV-CD8-FRB-ER -CS-Cre*, and *pCMV-CD8-FRB-ER-CS-Cre-EGFP*. To evaluate the effect of membrane-localized Cre, we generated *pCMV-CD8-FRB-CS-Cre* and *pCMV-CD8-FRB-CS-Cre-EGFP*.

We first evaluated the labeling efficiency and leakiness of the classical CreER-*loxP* system in an *in vitro* model by transfection in Ad293 cells (Figure 2A). Quantitative analysis of the data showed a 51.6%–79.7% labeling at 24–48 h after induction, while the uninduced labeling was as high as 24.1%–58.3%, which was equivalent to a leakage of approximately 47.2%–74.1% (Figure 2B). This alarmingly high percentage of unintended labeling could be due to a transfection artifact, for example, a recombination of the Cre reporter construct in the cytoplasm or extraordinary copy numbers of plasmid DNA.

We therefore generated a Cre reporter line of Ad293 cells (Ad293CR), which possesses a single copy of the Cre reporter in the genome (Figure S2). The labeling of Ad293CR cells with CreER was examined by both fluorescence microscopy and flow cytometry (Figures 2C, S3A, and S3B). The data confirmed the extremely high degree of leakiness, although the labeling efficiency was at a lower level (Figure 2D). When different amount of plasmid DNA was used, the leakage of

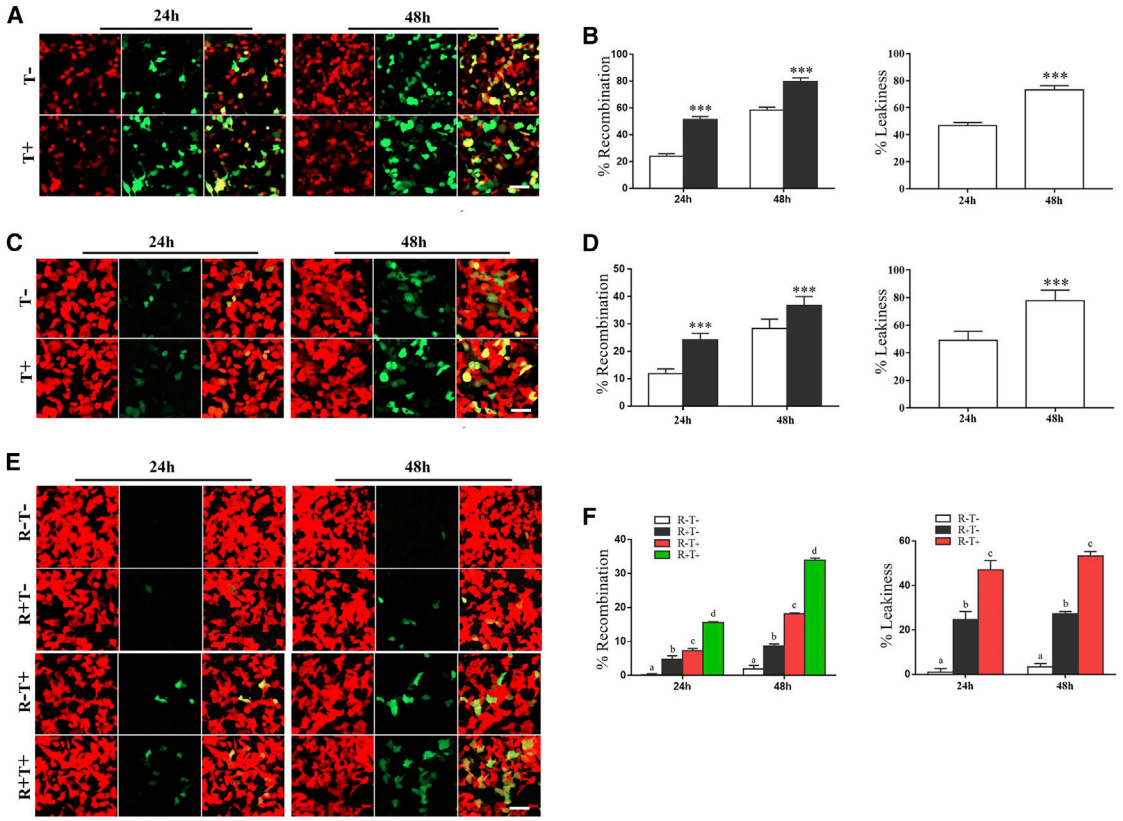

Figure 2. The dual inducible CreER system has a tight cell labeling capacity

(A) Ad293 cells were co-transfected with *pCMV-CreER* and the Cre reporter. Tamoxifen (T) was added 24 h after transfection. Microphotographs show the expression of dsRed or EGFP at 24 h and 48 h after induction in Ad293 cells. Scale = 50 μm. (B) Quantitative analysis of recombination rate and leakiness of CreER in Ad293 cells. Recombination rate (white bars = uninduced, black bars = induced) was calculated as the percentage of EGFP + cells vs. total fluorescently positive cells. Leakiness was calculated as the ratio between uninduced and induced recombination rate. Data are represented by mean ± standard error of the mean. n = 12. *** $p < 0.001$. (C) Ad293CR cells (Ad293 clone stably transfected with the Cre reporter) were transfected with *pCMV-CreER*. Microphotographs show the expression of dsRed or EGFP at 24 h and 48 h after induction in Ad293CR cells. Scale = 50 μm. (D) Quantitative analysis of recombination rate and leakiness of CreER in Ad293CR cells. Data are represented by mean ± standard error of the mean. n = 12. *** $p < 0.001$. (E) Ad293CR cells were co-transfected with *pCMV-mCreER* and *pCMV-mTEVp*. Rapamycin (R) and/or tamoxifen (T) were added at 24 h post transfection. Scale = 50 μm. (F) Cells in (E) were harvested and analyzed by flow cytometry. Bar graphs show recombination rate and leakiness of mCreER in Ad293CR cells. Leakiness was calculated as the percentage of recombination rate of no induction (R-T-) or single induction (R + T-, R-T+) vs. that of dual induction (R + T+). Data are represented by mean ± standard error of the mean. n = 12. Bars denoted with a different letter on top are significantly different ($p < 0.05$).

CreER in Ad293CR cells did not reduced to acceptable levels, and still maintained at about 36.2%–70.7% (Figure S4). Last, we generated two Ad293 clones stably expressing CreER (Ad293CreER), which also showed similar leakiness when transfected with the Cre reporter (Figure S5).

The labeling of Ad293CR cells with the dual inducible CreER-*loxP* system was then examined by both fluorescence microscopy and flow cytometry (Figures 2E and S3C). Labeling was rarely detectable in the absence of rapamycin and tamoxifen. Induction with rapamycin, tamoxifen, or both led to a labeling of 4.8%–8.5%, 7.3%–18.0%, and 15.6%–33.9% respectively in Ad293CR cells. This was equivalent to a leakage of about 4.7% without induction, 27.3% with rapamycin and 50.3% with tamoxifen at 48 h after induction (Figure 2F).

mCreER reduces the level of nuclear translocation

To detect directly the leakage of CreER into the nucleus, we fused an EGFP fragment C-terminally to CreER (Figure 1B). When produced in Ad293 cells, a measurable amount of CreER-EGFP appeared in the nucleus in the absence of induction as well as in the presence of tamoxifen (Figure 3A), and the nucleus EGFP signal increased dramatically from 24 h to 48 h. Quantitative analysis showed that uninduced nucleus EGFP reached 45.1%–79.5% of that of induced (Figure 3B), which was comparable to the level of leakiness of cell labeling with CreER (Figure 2B).

Similarly, we constructed an mCreER-EGFP fusion protein (Figure 1B). mCreER-EGFP appeared predominantly in the plasma membrane, while barely detectable in the nucleus in the absence of rapamycin and tamoxifen (Figure 3C). Induction with rapamycin,

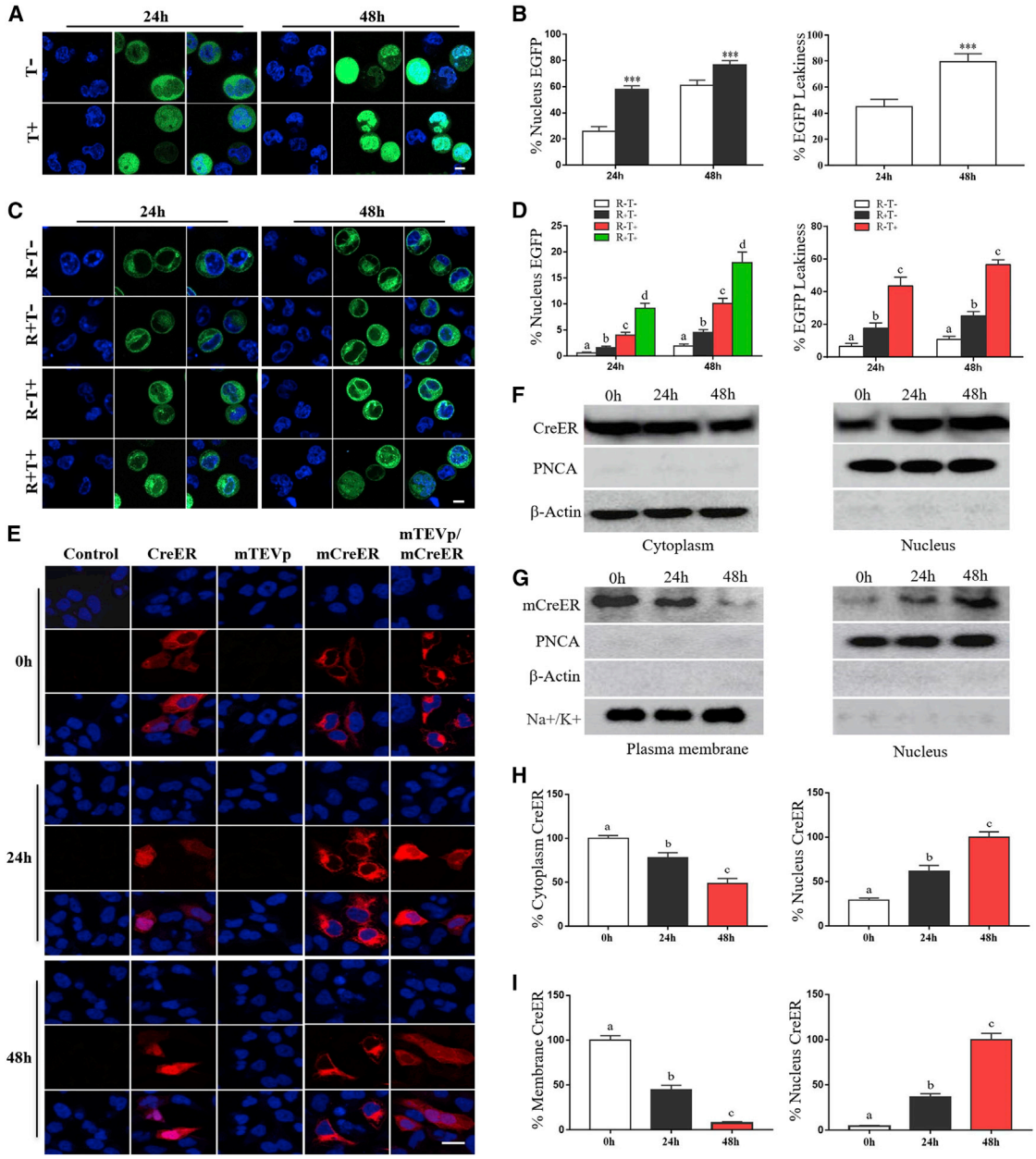

Figure 3. mCreER does not leak into the nucleus

Ad293 were transfected with *pCMV-CreER-EGFP* (A) or with *pCMV-mCreER-EGFP* (C). Tamoxifen (T) and/or rapamycin (R) were added 24 h after transfection. Micrographs show the intracellular distribution of CreER-EGFP (A) and mCreER-EGFP (C) at 24 h and 48 h after induction. Scale = 20 μm. Quantitative analysis of EGFP percentage in the nucleus and leakiness of CreER-EGFP (B) and mCreER-EGFP (D) in Ad293 cells. In (B), white bars = uninduced, black bars = induced. EGFP leakiness was calculated as the ratio between uninduced *vs.* induced nucleus EGFP. Data are represented by mean ± standard error of the mean. n = 48. *** $p < 0.001$. In (D), Leakiness was calculated as the percentage of recombination rate of no induction (R-T-) or single induction (R + T-, R-T+) vs. that of dual induction (R + T+). Data are represented by mean ± standard error of the mean. n = 48. Bars denoted with a different letter on top are significantly different ($p < 0.05$). (E) Ad293 cells were transfected with *pCMV-CreER*, *pCMV-mCreER*, *pCMV-mTEVp* or *pCMV-mCreER/pCMV-mTEVp*. After induction for 0, 24, or 48 h, cells were stained with anti-Cre antibody (red) and Hoechst (blue), and analyzed by confocal microscopy. Scale = 50 μm. (F, G) Ad293 cells were transfected with *pCMV-CreER* (F), or with *pCMV-mCreER/pCMV-mTEVp* (G). Induction was carried out at 24 h after transfection. Western blots show the distribution of CreER in the membrane, cytoplasm or nucleus at 0, 24, or 48 h after induction. (H and I) Semi-quantitative analysis of the percentage of CreER in the membrane, cytoplasm or nucleus in (F) and (G), respectively. For densitometric analysis, cytoplasmic or membrane localized CreER at 0 h was set as 100%, while nuclear CreER at 48 h after induction was set as 100%. β-Actin, Na^+/K^+ channel and PCNA were used for normalization and confirmation of the cytoplasm, plasma membrane and nucleus fractions, respectively. Data are represented by mean ± standard error of the mean. n = 6. In (D), (H) and (I), bars denoted with a different letter on top are significantly different ($p < 0.05$).

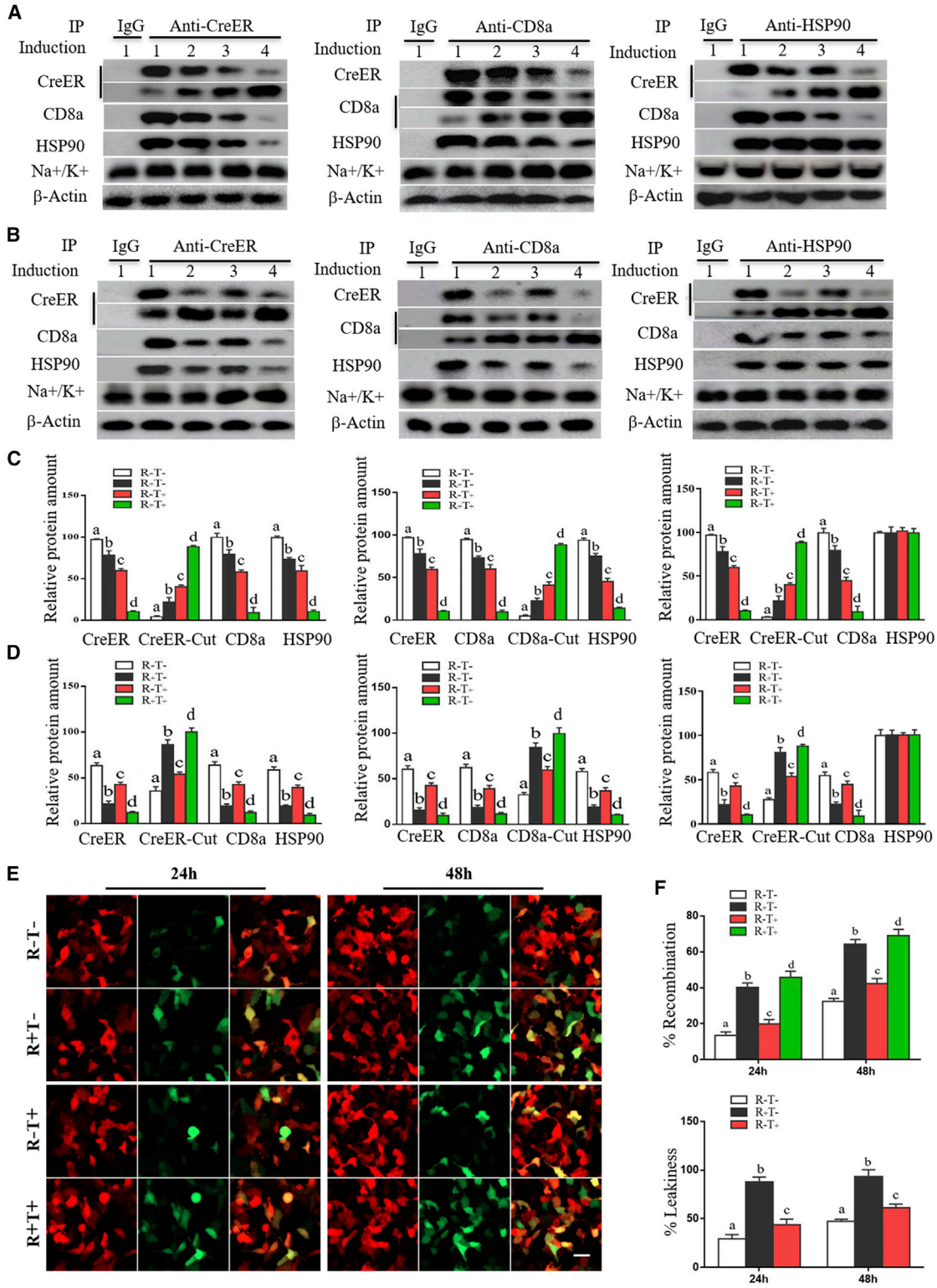

Figure 4. HSP90 is indispensable to the tightness of the dual inducible CreER system

(A) Ad293 cells were transfected with *pCMV-mCreER/pCMV-mTEVp*. Inducers (1: R-T-, 2: R-T+, 3: R + T-, 4: R + T+) were added at 24 h after transfection. Cells were harvested at 24 h after induction and used for immunoprecipitation/western blot (IP/WB) analysis. (B) HSP90 was knocked down in Ad293 cells by siRNA. Cells were

(legend continued on next page)

tamoxifen, or both led to 1.6%–4.5%, 4.0%–10.1%, and 9.2%–17.9%, respectively, of CreER-EGFP into the nucleus. In terms of CreER-EGFP leakiness, it was equivalent to approximately 6.4%–9.8% without induction, 17.7%–25.0% with rapamycin, and 43.6%–56.6% with tamoxifen at 24–48 h after induction (Figure 3D). The results were consistent with that of cell labeling with mCreER (Figures 2E and 2F), showing a dramatically reduced level of leakage.

We were curious about the role of the endoplasmic reticulum (ER) to the tightness of mCreER and, therefore, constructed several fusion proteins, in which the ER was fused N-terminally to Cre, or a TEVp CS was introduced in between the ER and Cre, or the ER was deleted all together (Figure S1). All these permutations led to leakiness to certain degree (Figures S7–S9), revealing a CS-CreER arrangement was critical to the tightness of cell labeling.

Furthermore, immunofluorescence staining with anti-Cre antibody confirmed the appearance of CreER in the nucleus in the absence of tamoxifen, while mCreER clearly located exclusively in the plasma membrane (Figure 3E). mCreER translocated to the nucleus only in the presence of mTEVp with induction. Moreover, a Western blot analysis was carried out to probe the cellular distribution of CreER and mCreER (Figures 3F and 3G). The purified nucleus and cytoplasm fractions were verified by the PNCA and beta-actin staining respectively, while the plasma membrane fraction was confirmed by Na^+/K^+ pump staining. Semi-quantitative densitometry analysis showed that the percentage of nucleus CreER was as high as 28.9% in Ad293 cells expressing the classical CreER in the absence of induction, while the percentage decreased to 4.6% when the mCreER was used (Figures 3H and 3I).

Association of HSP90 with mCreER decreases unintended cleavage by mTEVp

The above experiments repeatedly showed that the induction effect of tamoxifen was greater than that of rapamycin, and the combined effect of rapamycin and tamoxifen was slightly greater than the sum of individual inducer (Figures 2 and 3). Since the ER was critical to the tightness of mCreER, we thought that ER in the plasma membrane could be associated with HSP90, which is similar with the cytoplasmically located counterpart. A western blot experiment was performed to test this hypothesis, showing indeed HSP90 could co-immunoprecipitated with mCreER or CD8α (Figure S10A). Further, addition of tamoxifen induced dissociation of more than 84.8% of HSP90 from mCreER at 24 h after induction (Figure S10B).

In the presence of mTEVp, mCreER was cut and CreER was released from the membrane in the presence of rapamycin and/or tamoxifen at 24 h (Figure 4A). The percentage of CreER cut from mCreER was quantified by densitometry analysis, which showed about 4.3% for non-induction, 22.0% for rapamycin, 40.3% for tamoxifen, and 88.6% for both rapamycin and tamoxifen (Figure 4C).

The results suggested that the association of HSP90 might have blocked the TEVp CS in mCreER, and thus prevented unintended cleavage of CreER from the plasma membrane. To test this possibility, small interfering RNA (siRNA) was used to knockdown the level of HSP90 in Ad293 cells. The protein and transcript level of HSP90 reduced to about 17.3% and 10.1%, respectively, at 72 h after transfection (Figure S11).

In contrast, after HSP90 knockdown, we found mCreER was cut in measurable amount even in the absence of induction (Figure 4B). A quantitative analysis showed that approximately 35.6% CreER released from the membrane for non-induction, 86.2% for rapamycin, 53.9% for tamoxifen, and 99.5% for both rapamycin and tamoxifen (Figure 4D). The results clearly demonstrated that, at the reduced level of HSP90, the unintended cleavage of mCreER increased dramatically and, thus, abolished largely the tightness of the dual inducible system (Figures 4E and 4F).

mCreER reduces the level of cytotoxicity

Dozens of cryptic *loxP* sites have been reported, and cleavage of these cryptic *loxP* sites could damage the genome and produce unwanted phenotypes in Cre driver lines.[15,30–32] We found that transfection of CreER led to a reduced viability in Ad293 cells after induction with tamoxifen for 24–48 h (Figure 5A). The expression of mCreER alone did not affect cell proliferation, only transfection of both mCreER/mTEVp constructs decreased cell viability at 48 h after induction, but not as severe as that transfection with CreER plasmid, suggesting that membrane localization of CreER could reduce cytotoxicity.

A cell cycle analysis by flow cytometry was then carried out to investigate the exact cell cycle stage being affected (Figure S12). The data showed that the expression of CreER increased the percentage of cells in G1 stage and decreased the percentage of cells in the G2/M stages (Figures 5B–5D). A detailed comparison of the cell cycle stage showed that CreER decreased cells in G2/M stage even in the absence of tamoxifen. mCreER also affected cell cycle progression, but not as severely as CreER.

We then measured genome damage by western blot (Figure 5E) and immunostaining of γ-H2AX (Figure 5G), which has been shown to be bound to DNA breakage sites.[33] The result showed that the γ-H2AX

reseeded in six-wells at 48 h, and then co-transfected with *pCMV-mCreER/pCMV-mTEVp*, IP/WB analysis was carried out at 24 h after induction. For CreER and CD8α, the upper and lower bands represent membrane bound and cleaved protein species, respectively. Semi-quantification of protein density was shown in (C) and (D). Data are represented by mean ± standard error of the mean. n = 3. (E) HSP90-knockdowned Ad293 cells were co-transfected with *pCMV-mCreER*, *pCMV-mTEVp* and the Cre reporter. Inducers were added 24 h after transfection. Scale = 50 μm. (F) Quantitative analysis of the recombination rate and leakiness of mCreER in Ad293 cells after HSP90 knockdown. Data are represented by mean ± standard error of the mean. n = 12. In (C), (D), and (F), bars denoted with a different letter on top are significantly different ($p < 0.05$).

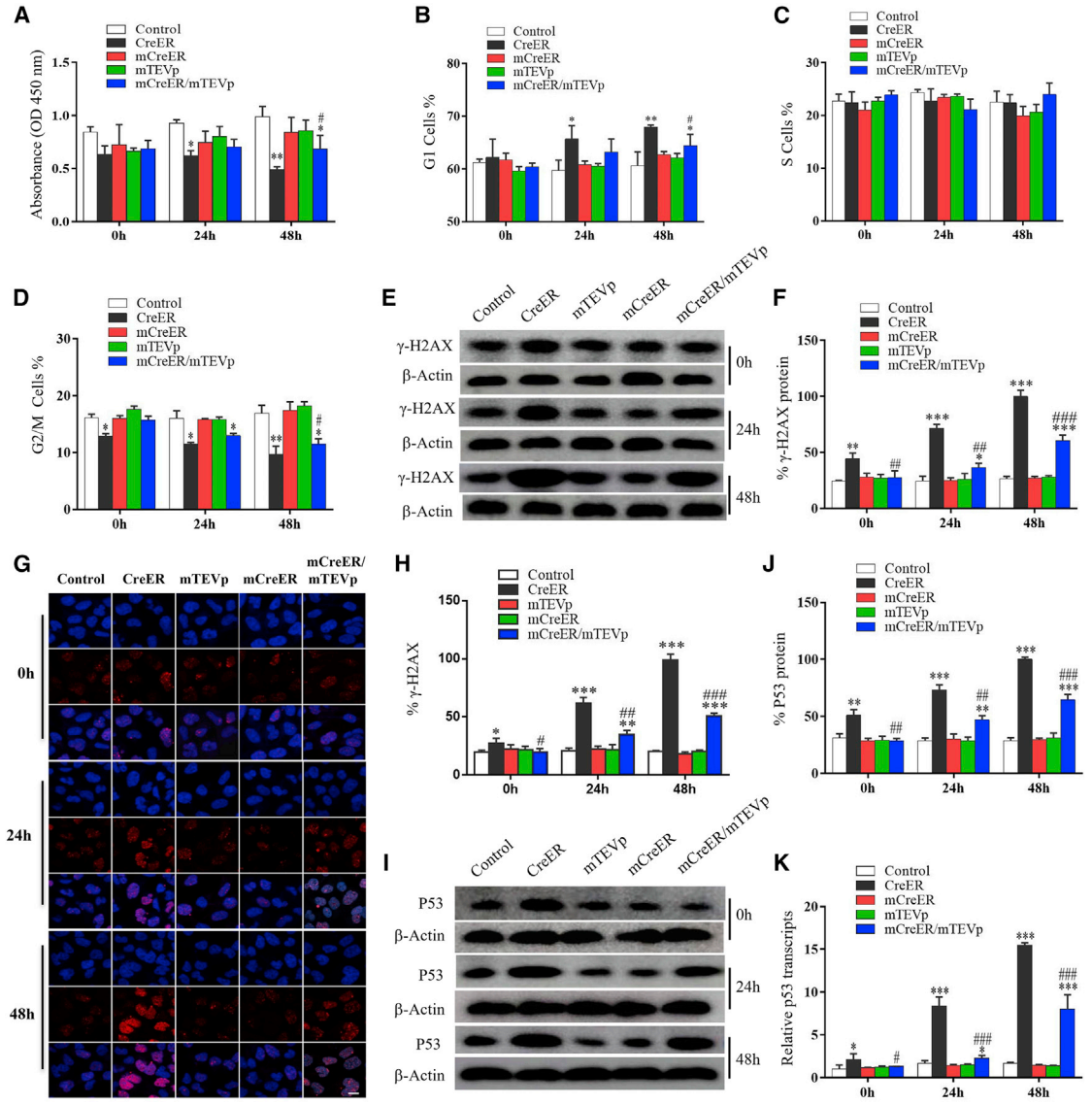

Figure 5. The dual inducible CreER system has low cytotoxicity

Ad293 cells were transfected with *pCMV-CreER*, *pCMV-mCreER*, *pCMV-mTEVp* or *pCMV-mCreER/pCMV-mTEVp*. The control group was transfected with the vector backbone. Inducers were added at 24 h after transfection. Cells were analyzed at 0, 24, or 48 h after induction. (A) Cell viability was measured using the CCK-8 assay. (B–D) After staining with propidium iodine (PI), DNA content and cell cycle analysis was performed using flow cytometry. The proportion of cells in G1, S, and G2/M stages was determined using the Modfit software. Data are represented by mean ± standard error of the mean. n = 3. (E) γ-H2AX protein was detected by western blotting. (F) Semi-quantitative analysis of γ-H2AX protein density. Data are represented by mean ± standard error of the mean. n = 6. (G) Immunofluorescence staining of γ-H2AX (red) and Hoechst (blue) in transfected cells. (H) Semi-quantitative analysis of γ-H2AX signal. The relative intensity of γ-H2AX in cells expressing CreER at 48 h was set as 100 (black bar). Data are represented by mean ± standard error of the mean. n = 12. (I) Western blot analysis of P53 protein. (J) Semi-quantitative analysis of P53 protein density. The relative intensity of P53 (normalized with β-actin) in cells expressing CreER at 48 h was set as 100 (black bar). Data are represented by mean ± standard error of the mean. n = 3. (K) Quantitative real-time RT-PCR analysis of *p53* transcript levels. β-Actin was used for normalization. Data are represented by mean ± standard error of the mean. n = 3. The significant difference to the control is denoted with * $p < 0.05$, or *** $p < 0.001$; significant difference between CreER and mCreER/mTEVp is denoted with # $p < 0.05$.

protein level increased in Ad293 cells transfected with CreER plasmid, even in the absence of tamoxifen (Figure 5F). The protein level of γ-H2AX increased also in Ad293 cells transfected with mCreER plasmid, but only in the presence of induction, and the level was significantly lower than that transfected with CreER plasmid. The percentage of cells stained positive for γ-H2AX was consistent with that of γ-H2AX protein levels (Figure 5H). Last, the protein and transcript levels of p53 were determined by western blot (Figures 5I and 5J) analysis and quantitative reverse transcriptase PCR (Figure 5K). The results showed a similar pattern with that of γ-H2AX.

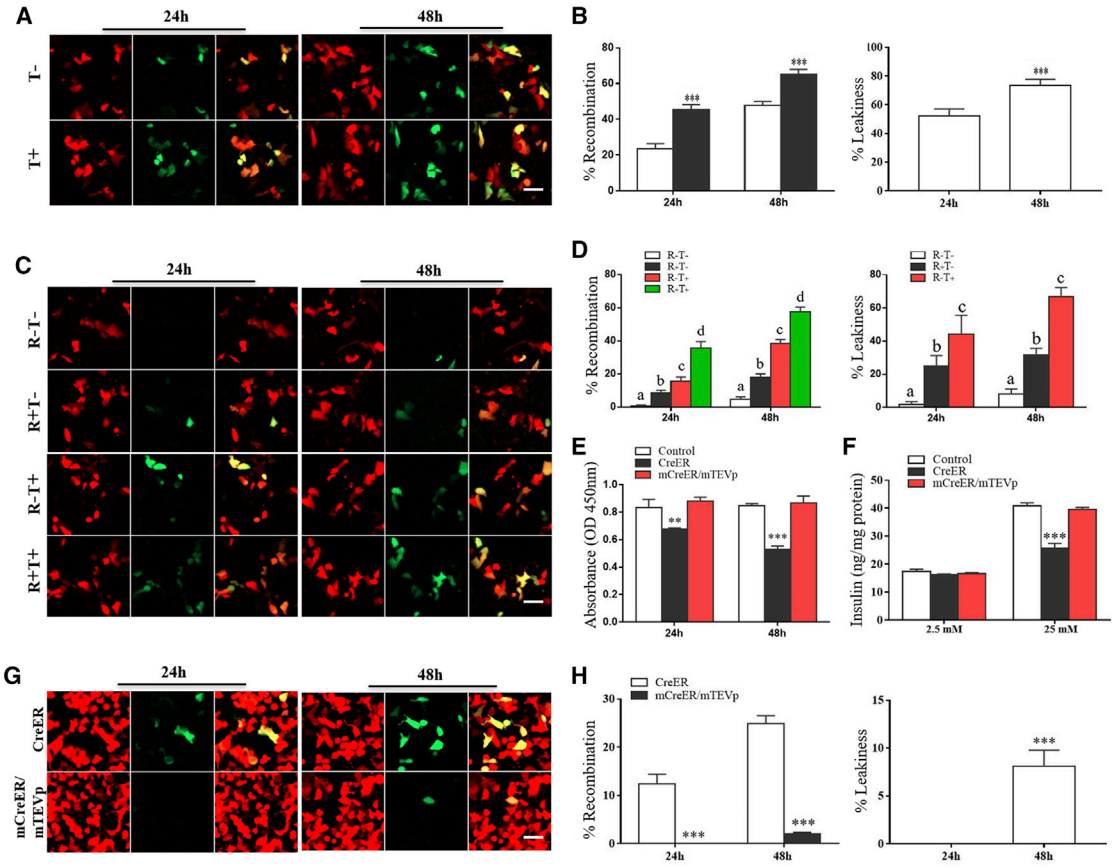

Figure 6. High quality labeling of islet beta-cells with the dual inducible CreER system

(A) MIN6 islet beta-cells were infected with lentiviral particles (MOI = 10) carrying a RIP-CreER expression cassette (*Lenti-RIP-CreER*). (C) MIN6 cells were infected with *Lenti-RIP-mCreER and Lenti-RIP-mTEVp* (MOI = 10). (G) Ad293 cells were infected with *Lenti-RIP-CreER*, or infected with *Lenti-RIP-mCreER and Lenti-RIP-mTEVp* (MOI = 10). MIN6 or Ad293 cells were simultaneously transfected with the Cre reporter. Tamoxifen and/or rapamycin were added 24 post infection/transfection. Scale = 50 μm. (B, D, H) The recombination rate and leakiness were determined at 24 h or 48 h post induction. Data are represented by mean ± standard error of the mean. n = 12. ***, $p < 0.001$. (E) MIN6 cells were infected with *Lenti-RIP-CreER* or co-infected with *Lenti-RIP-mCreER* and *Lenti-RIP-mTEVp*. The control group was infected with *Lenti-CMV-EGFP*. Cell viability was measured using the CCK-8 assay. (F) MIN6 cells were infected as in (E). Insulin secretion in media with low glucose (2.5 mM) or high glucose (25 mM) was measured using ELISA. Data are represented by mean ± standard error of the mean. n = 6. ***, $p < 0.001$.

RIP promoter-driven mCreER provides superior labeling in islet beta-cells

To verify the above findings in MIN6 islet beta-cells of mice, we produced lentiviral particles carrying an expression cassette of CreER, mCreER, or mTEVp driven by the RIP promoter, which is the most widely used promoter in generating CreER driver lines for beta-cell tracing. The transduction of MIN6 cells with *Lenti-RIP-CreER* simultaneously with transfection of the Cre reporter revealed substantial levels of labeling, even in the absence of tamoxifen (Figure 6A). The level of leakage (52.2%–73.5%) was comparable with that in Ad293 cells (Figure 6B).

In contrast, the transduction of MIN6 cells with *Lenti-RIP-mCreE/Lenti-RIP-mTEVp* showed minimal levels of labeling (Figure 6C). Quantitative analysis showed a leakiness of 8.0% without induction, 31.6% with rapamycin and 66.9% with tamoxifen at 48 h after induction (Figure 6D), which were a little bit higher than that in Ad293 cells.

The cytotoxicity of CreER in MIN6 cells was first evaluated by CCK-8 assay. The result showed that the transduction of *Lenti-RIP-CreER* decreased cell proliferation significantly, while transduction of *Lenti-RIP-mCreE/Lenti-RIP-mTEVp* did not affect cell viability (Figure 6E). Furthermore, transduction with *Lenti-RIP-CreER* but not with *Lenti-RIP-mCreE/Lenti-RIP-mTEVp* significantly decreased insulin secretion at 25 mM glucose (Figure 6F). The insulin content of MIN6 cells was not affected by the transduction of either *Lenti-RIP-CreER* or *Lenti-RIP-mCreE/Lenti-RIP-mTEVp* (Figure S13).

Finally, Cre driver lines with RIP promoter frequently showed non-specific labeling of cells other than islet beta-cells, especially under pathological conditions.[34,35] We interrogated this problem by

expressing mCreER in Ad293 cells (Figure 6G), which are not insulin-producing cells. As expected, transduction with *Lenti-RIP-CreER* led to 12.4%–24.8% of cell labeling at 24–48 h after induction (Figure 6H). In contrast, transduction with *Lenti-RIP-mCreE*/*Lenti-RIP-mTEVp* led to the labeling of a few Ad293 cells at 48 h after induction, which was only 7% compared with that with *Lenti-RIP-CreER* (Figures 6G and 6H).

DISCUSSION

To improve the temporal and spatial controllability of the Cre-*loxP* system, numerous innovations have been reported. One common strategy is to split the Cre recombinase in half into N-terminal and C-terminal fragments (NCre and CCre, respectively). Under the control of different promoters, the expression of NCre and CCre in the same cell can combine and recover recombination activity.[36] Alternatively, NCre and CCre are fused to different photoreceptors, which are light activatable and, thus, enables optogenetical regulation of genome engineering.[37,38]

The above manipulations greatly increase the tunability; however, the issue of the leakiness of CreER remains unsolved to this day. Reducing the expression level of CreER by using a weaker promoter or increase of the distance between two *loxP* sites could help to decrease the uninduced recombination; however, this is achieved with the compensation of labeling efficiency.[11,12] Adding another ER domain to the N-terminus of Cre (MerCreMer or ERT2CreERT2) clearly improves the labeling stringency.[39,40] This strategy anyway does not provide additional mechanisms for tethering Cre in the cytoplasm, and a greater amount of tamoxifen might be needed to induce nucleus translocation. Nonetheless, various degrees of leakiness have been reported in the brain and skeletal muscle of MerCreMer transgenic mice.[41,42]

Our *in vitro* system revealed an extraordinary level of unintended cell labeling activity of CreER (Figures 2A and 2B), which is much higher than that reported in most of *in vivo* studies (Table S4). This sensitive system allows us to detect even a slight improvement in the leakiness with CreER modifications. Indeed, membrane tethering of CreER decreased the background labeling to about 4.7% (Figures 2E and 2F). Compared with that of 74.1% with the classical CreER, this is approximately a 15.7-fold reduction in leakage. Notably, this outstanding feature of mCreER was not obtained by compromising labeling efficiency, which showed a comparable labeling activity of more than 90% in Ad293 cells (Figures S5 and S6), approximately 35% in Ad293CR cells (Figures 2C and 2F) and 60% in MIN6 islet beta-cells (Figures 6A and 6C). In comparison, we found a significant amount of unintended labeling in Ad293 and Ad293CR cells, even when the ERT2CreERT2 construct was used (Figure S14).

We showed definitively that CreER cell labeling leakiness was due to uninduced nuclear translocation (Figures 3A and 3E). A couple of mechanisms are probably accountable for this phenomenon. CreER, as a fusion protein of Cre with the estrogen receptor ligand binding domain (ER), its anchorage in the cytoplasm depends solely on the binding with the cytoplasmically located HSP90.[43] The overexpression of the CreER transgene, or the lack of HSP90 protein due to excessive requirement under stress conditions, might release some CreER from anchorage. Another possibility—disassembly of the nucleus envelop during mitosis—might expose chromosomal DNA to CreER. Membrane location of CreER solves all these problems; and indeed, mCreER is tightly bound to the membrane under uninduced conditions (Figures 3C and 3E).

This membrane-localized CreER incorporates the chemically induced dimerization machinery and is dual inducible with rapamycin and tamoxifen. Further, mCreER alone (in the absence of mTEVp) could not produce any cell labeling even in the presence of tamoxifen (data not shown). mTEVp is indispensable for the release of CreER from the plasma membrane. Ideally, the system is activated only in the presence of both inducers; however, a single inducer of rapamycin or tamoxifen could lead to substantial cell labeling. This is likely due to self-dimerization of the CD8α chain[44] or the existence of unknown serum-borne ligand(s) with a similar activity of rapamycin or tamoxifen. Nonetheless, leakiness in the presence of a single inducer does not affect the practical use of this dual inducible CreER system for lineage tracing.

An unexpected observation of this system is the synergetic effects between rapamycin and tamoxifen, suggesting tamoxifen may help in CreER cleavage, in addition to the induction of nucleus translocation. This synergy depends critically on the expression of HSP90, since its knockdown dramatically reduced the labeling tightness (Figures 4E and 4F). The results suggested that HSP90 binds to the membrane localized CreER and is in such a conformation, which accidentally conceals the TEVp CS. The presence of tamoxifen induces change of conformation of CreER and exposes the CS and thus allows the cleavage by TEVp. This hypothesis was further confirmed by changing the position of ER or deletion of the ER fragment from mCreER fusion protein, which affected significantly the labeling tightness (Figures S7–S9).

In addition to the labeling tightness, this dual inducible CreER system has other superior features, such as low cytotoxicity (Figure 5) and labeling specificity (Figure 6). CreER produces a double-strain break on DNA, which counts as a genome damage. If the breakage persists due to the constant presence of CreER in the nucleus, the cell will be blocked in the G1 stage and will initiate the DNA damage repair pathway,[33] such as an increased expression of γH2AX and p53, and formation of the DNA repair foci (Figure 5). Low cytotoxicity of mCreER in MIN6 islet beta-cells preserved not only cell viability but also insulin content and secretion in response to high glucose concentration (Figures 6 and S13). Last, RIP specificity was improved by using mCreER (Figure 6G). We believe this is likely achieved via lowering the protein amount in the plasma membrane (mCreER) compared with the cytoplasmic counterpart (CreER).

A disadvantage of this system in several aspects is immediately noticeable. An extra construct for the expression of mTEVp is needed to

implement this bipartite cell labeling scheme. Laborious as it seems to be, we have successfully produced transgenic mice (three F1 mice to this day) carrying islet beta-cell-specific mTEVp/mCreER expression constructs without extra cost and effort (data not shown). Transgenic expression of TEVp has been reported in drosophila, confirming that TEVp is not deleterious to the development.[45,46] Chemically induced dimerization including the FKBP/FRB has been well implemented in transgenic mice.[47,48] The administration of rapamycin could be a serious concern to studies of embryonic development. Nevertheless, synthetic substitutes for rapamycin that do not interfere with endogenous signaling have been generated.[49,50]

In summary, membrane localization of CreER prevents unintended entry into the nucleus. When grafted with the chemically induced dimerization machinery, the cleavage of mCreER and subsequent nuclear translocation could be induced sequentially by rapamycin and tamoxifen. This system has an extremely low cell labeling leakage and cytotoxicity without compromising labeling efficiency. Although has not been tested in *in vivo* study, this novel dual inducible CreER system will be invaluable to cell lineage tracing and genome engineering in a more precisely temporal and spatial controllable manner.

MATERIALS AND METHODS

Plasmid construction

All plasmids were generated from *pCMV-EGFP-N1* of Clontech (Mountain View, CA), *pCMV-CD8-EGFP*[51], *pCMV-FKBP-LD0-TEVp*, *pCMV-FRB-LD0-tTA-BFP*[52] of Addgene (Cambridge, MA) and *pCMV-CreER* (*CreERT2* abbreviated as *CreER*, preserved in our laboratory) using standard cloning techniques as described below, and verified by sequencing by Sangon (Shanghai, China).

The following conditions were used in all PCR reactions: 100–300 pg of DNA template, 2×Taq PCR Master mix (TianGen Beijing) and 0.2 μM primers in a total reaction volume of 20 μL. Thermocycle parameters were: 95°C for 3 min, followed by 95°C for 10 s, 60°–65°C for 30 s and 72°C for 1 min for a total of 30 cycles. Sequences of primer sets are listed in Table S1.

Construction of pCMV-mCreER (pCMV-CD8-FRB-CS-CreER)

EGFP was deleted from *pCMV-CD8-EGFP* by cutting with SmaI and NotI, the vector backbone was recovered and ligated with the CreER fragment, which was PCR amplified from *pCMV-CreER* with primers F1/R1 containing SmaI/NotI at 5′-ends. The FRB-CS fragment was PCR amplified from *pCMV-FRB-LD0-tTA-BFP* with primers F2/R2 containing EcoRI/SmaI at 5′-ends. The CS sequence (TEV CS: 5′-gaaaacctgtattttcagggt-3′) was introduced into the R2 primer after SmaI. The FRB-CS fragment was then inserted between CD8 and CreER, which generated *pCMV-mCreER* (*pCMV-CD8-FRB-CS-CreER*) encoding a membrane localized CreER.

Construction of pCMV-mCreER-EGFP

pCMV-CD8-EGFP was cut with EcoRI and SacII between CD8 and EGFP. The FRB-CS-CreER fragment was PCR amplified from *pCMV-mCreER* with primers F3/R3 containing EcoRI/SacII at the 5′-ends, and then ligated to *pCMV-CD8-EGFP* at EcoRI/SacII.

Construction of pCMV-mTEVp (pCMV-CD8-FKBP-TEVp)

EGFP was deleted from *pCMV-CD8-EGFP* by cutting with BamHI and NotI, and the vector backbone was recovered and ligated with the TEV protease (TEVp) fragment, which was PCR amplified from *pCMV-FKBP-LD0-TEVp* with primers F4/R4 containing BamHI/NotI at the 5′-ends. The FKBP fragment was PCR amplified from *pCMV-FKBP-LD0-TEVp* with primers F5/R5 containing BamHI/EcoRI at the 5′-ends, respectively. The FKBP fragment was then inserted between CD8 and TEVp, which generates *pCMV-mTEVp* (*pCMV-CD8-FKBP-TEVp*), expressing a membrane localized TEV protease.

Construction of pCMV-CreER-EGFP

The CreER fragment was PCR amplified from *pCMV-CreER* with primers F6/R6 containing NheI/EcoRI at the 5′-ends and then ligated in frame to *pCMV-EGFP-N1*, which had been cut with NheI/EcoRI between the CMV promoter and EGFP.

Cell culture

All cell lines, including Ad293, Ad293CR, Ad293CreER (generated from Ad293 cells by transduction of lentiviral particles carrying a CreER expression cassette), and MIN6 were cultured in DMEM (Life Technologies, Rockville, MD) supplemented with 10% fetal calf serum (HyCLONE, Logan, UT), 2 mM glutamine, 50 U/mL penicillin G sodium, and 50 μg/mL streptomycin sulfate (Beyotime, Haimen, China). Cells were cultivated in a humidified incubator at 37°C supplied with 5% CO_2.

Cell transfection

For each 96-well, DNA (50 ng) and 0.3 μL of Polyjet reagent (SignaGen Laboratories, Rockville, MD) were diluted in 5 μL PBS. Polyjet reagent was then added into DNA, vortexed three times, and incubated at room temperature for 15 min. The DNA complexes was then mixed with 100 μL culture medium and added into a 96-well that had been pre-seeded with respective cells. DNA complexes were removed at 12 h and fresh culture medium was replenished. Rapamycin (100 μM) and/or tamoxifen (5 μM) were added at 24 h after transfection. Cells stained with or without Hoechst (10 μg/mL) were imaged at 24 h and 48 h after induction using a fluorescence microscope equipped with a CCD camera (Zeiss Axio Imager M2, Carl Zeiss, Germany). Alternatively, cells were harvested and transferred to a 35-mm glass bottom dish, and examined under a confocal microscope (Zeiss LSM 800, Carl Zeiss, Germany) using a 63× objective.

Calculation of recombination rate and leakiness

Ad293 cells or MIN6 cells expressing dsRed or EGFP were examined under a fluorescence microscope (Zeiss Axio Imager M2, Carl Zeiss, Jena, Germany). Five evenly distributed images from each 96-well were taken. For every experiment each condition was measured in triplicate, and each experiment was repeated at least three times. Twelve pictures were selected randomly for quantification analysis.

EGFP + or dsRed + cell number was determined using Image-Pro Plus software (Media Cybernetics, Rockville, MD). The recombination rate was calculated as the percentage of EGFP + cells vs. the total fluorescently positive cells in each picture. Leakiness was calculated as the ratio between the uninduced and the induced recombination rates. For experiments using the CreER-EGFP or mCreER-EGFP fusion protein, cells were harvested, put into a 35-mm glass-bottom dish, and examined under a confocal microscope (Zeiss LSM 800, Carl Zeiss) using a 63× objective. Microphotographs in five positions (left, right, up, down, meddle) were taken. Each experimental condition was performed in six 96-wells. At least two cells from each randomly selected 24 pictures were used for quantification analysis using Image-Pro Plus software (Media Cybernetics). The nucleus or the whole cell was circled manually, and the respective integrated fluorescence intensity were determined. The nucleus EGFP rate was calculated as the percentage of nucleus EGFP vs. the total EGFP in each cell. EGFP leakiness was calculated as the ratio between the uninduced vs. the induced nucleus EGFP rate.

Western blotting

Protein purification was carried out using a Nuc-Cyto-Mem Preparation Kit according the instruction provided by the company (APPLYGEN, Beijing, China). Ad293 cells seeded overnight in six-wells were transfected with *pCMV-CreER*, *pCMV-mCreER/pCMV-mTEVp*, or under the indicated conditions. Tamoxifen and/or rapamycin were added at 24 h after transfection. Cells (1×10^7) were collected at 0 h, 24 h, and 48 h after induction. Cells were washed once with ice-cold PBS and resuspended in 0.5 mL of the Cytosol Extraction Reagent solution and transferred to an ice-cold Dounce homogenizer. Cells were homogenized on ice for 30–40 times and centrifuged at 800 *g* for 5 min at 4°C. The supernatant was transferred to a new 2-mL microcentrifuge tube, mixed with 50 μL Membrane Extraction Reagent solution, and centrifuged at 14,000 *g* for 30 min at 4°C. Supernatant was collected and used as the cytoplasm fraction, while the pellet was used as the membrane fraction. In addition, the pellet of the first centrifugation was resuspended in 500 μL of the Nuclear Extraction Reagent (solution) solution, centrifuged at 4,000 *g* for 5 min at 4°C. The pellet was washed once with 500 μL of NER and used as the nucleus fraction. The above extracted proteins from the membrane, cytoplasm and nucleus were mixed with 3× SDS loading buffer (Cell Signaling Technology, Beverly, MA), and heated to 100°C for 5 min before running in a 12% SDS PAGE gel. The protein concentration was determined by the BCA method to ensure equal amounts of total protein were added. After electrophoresis, the proteins were electo-transferred onto a PVDF membrane (MultiSciences, Hangzhou, China), blocked in 5% non-fat dry milk solution for 30 min, incubated with rabbit anti-Cre antibody, rabbit anti-phospho-histone H2A.X (Ser139) antibody, rabbit anti-P53 antibody, rabbit anti-HSP90 antibody (1:1,000, Cell Signaling Technology), rabbit anti-CD8a antibody (1:1,000, Abcam, Cambridge, UK), rabbit anti-β-actin antibody (1:1,000, Abbkine, Wuhan, China), or rabbit anti-Na+/K + ATPase antibody (1:1,000, Abbkine, Wuhan, China) overnight at 4°C. After washing three times for 5 min each time with TBST solution (Tris-Buffered Saline +0.1% Tween 20), the membrane was incubated with horseradish peroxidase-conjugated donkey anti-rabbit antibody (1:10,000, Sangon Biotech, Shanghai, China) for 1 h at room temperature. After washing three times, the membrane was developed using the enhanced chemiluminescence solution (ChemStudio SA, Thermo Fisher Scientific, Carlsbad, CA). Protein band intensity was quantified using Image-Pro Plus software (Media Cybernetics).

Co-immunoprecipitation

Ad293 cells seeded overnight in six wells (1×10^7) were transfected with *pCMV-mCreER*, tamoxifen was added at 24 h after transfection, cells were collected at 0 h, 8 h, 16 h, or 24 h after induction (Figure S8). Cells were transfected with *pCMV-mCreER/pCMV-mTEVp*, inducers (rapamycin and/or tamoxifen) were added at 24 h after transfection, cells were collected at 24 h after induction. Harvested cells were resuspended in 1000 μL of pre-cooled IP lysis buffer (20 mM Tris (pH 7.5), 150 mM NaCl, 1% Triton X-100; Beyotime). After incubation on ice for 10 min, cells were centrifuged at 12,000 *g* and 4°C for 10 min. Supernatant was collected, and protein concentration was determined by BCA method. A fraction of the supernatant was saved and used as input. For co-IP, supernatant containing 1 mg proteins was incubated with 2 μg specific or control IgG antibody at 4°C overnight with rotation, and then samples were mixed with 40 μL protein A + G agarose, incubated further at 4°C for 3 h with rotation. The samples were centrifuged at 2,500 *g* at 4°C, the pellet was then washed three times with IP lysis buffer, and proteins were eluted with 40 μL 1× loading buffer. Eluded proteins were detected by western blot assay or stored at −20°C before use.

RNA interference

The siRNA sequences targeting the messenger RNA of HSP90 and control have been reported previously (Table S2, [53]). The HSP90A, HSP90B, and control non-targeting siRNAs were purchased from Genscript (Nanjing, China). Cells in six-wells were transfected with respective siRNA (40 pmol) using 4 μL Pepmute Transfection Reagent (SignaGen Laboratories). The medium was replaced with fresh medium 12 h after transfection, and the whole cell lysate were prepared at 48 h or 72 h after transfection for western blot analysis. Alternatively, cells were collected for quantitative reverse transcriptase PCR analysis.

Cell viability assay

Cell viability was measured by using the Cell Counting Kit-8 (CCK-8) assay (Beyotime, Shanghai, China). Ad293 cells seeded overnight in 96-wells were transfected with *pCMV-CreER*, *pCMV-mTEVp*, *pCMV-mCreER*, or *pCMV-mCreER/pCMV-mTEVp*. Rapamycin and/or tamoxifen were added at 24 h after transfection. CCK-8 reagent was added at 0 h, 24 h, or 48 h after induction. After incubation at 37°C for 2 h, the optical density at 450 nm was determined with a microplate reader.

Flow cytometry analysis

Ad293 cells seeded overnight in 96-wells were transfected with *pCMV-CreER*, *pCMV-mTEVp*, *pCMV-mCreER*, or *pCMV-mCreER/pCMV-mTEVp*. Rapamycin and/or tamoxifen were added at 24 h

after transfection. Cells were collected after 24 h or 48 h induction. Samples from three 96-wells were pooled and applied to a BD FACSAria (Becton Dickinson, Franklin Lakes, NJ) equipped with a 70-mm nozzle. Dead cells and debris were excluded using FSC (forward scatter) and SSC (side scatter). A total of 10,000 events for each sample were acquired and analyzed with Flow Jo VX 10. Recombination rate was calculated as the percentage of EGFP-positive cells vs. total fluorescently positive cells. Leakiness was calculated as the ratio between the uninduced and the induced recombination rate.

DNA content was determined using the Cell Cycle and Apoptosis Analysis Kit (Beyotime, Shanghai, China). Cells from three 96-wells were harvested, washed one time with ice-cold PBS, and dispersed gently by vortexing. We added 1 mL ice-cold 70% ethanol drop by drop. After fixing at 4°C overnight, cells were incubated in staining solution containing 50μg/mL propidium iodine and 20 μg/mL RNase A at 37°C for 30 min. The sample was run in a BD FACSAria (Becton Dickinson). After exclusion of doublets, the analysis of cell cycle distribution was performed with ModFit LT 5.0 Software (Becton Dickinson).

Immunofluorescence cell staining

Ad293 cells seeded overnight in 96-wells were transfected with *pCMV-CreER*, *pCMV-mTEVp*, *pCMV-mCreER*, or *pCMV-mCreER/pCMV-mTEVp*. Rapamycin and/or tamoxifen were added at 24 h after transfection. Cells were then fixed at 0 h, 24 h, or 48 h after induction with 4% paraformaldehyde for 15 min at room temperature and permeabilized with 0.2% Triton X-100 for 10 min. Cells were incubated with the rabbit anti-H2A.X antibody (1:400, Cell Signaling Technology) or rabbit anti-Cre antibody (1:400, Cell Signaling Technology) for 2 h, and Cy3 goat anti-rabbit IgG (1:200, Beyotime, Shanghai, China) for 1 h, and finally with Hoechst 33,342 (10 μg/mL) (Beyotime, Shanghai, China) for 20 min. Three PBS washings were performed between each step. Images were taken under a fluorescence microscope equipped with a CCD camera (Nikon, Eclipse TE 2000, Tokyo, Japan).

Quantitative real-time RT-PCR

Total RNA was isolated by using TRIzol reagent according to the manufacturer's protocol. Reverse transcription was carried out using a ToloScript RT EasyMix for qPCR Kit according the instruction provided by the company (TOLO Biotech, Shanghai, China). Two-Step gDNA Erase-Out Mix added to 1 μg of the total RNA for the removal of residual DNA in a total volume of 16 μL at 42°C for 2 min. ToloScript qRT EasyMix added to above reaction production used for the reverse transcription in a total volume of 20 μL 37°C for 15 min. After reverse transcription, the cDNA was diluted with H_2O into a volume of 100 μL, of which 5 μL was used in real-time PCR for *P53*, *HSP90*, and *ß-actin* measurement. Sequences of specific primers are presented in Table S3. PCR was carried out in a 96-well plate using the LightCycler480 system (Roche, Indianapolis, IN) with the following thermal conditions: 95°C for 5 min followed by 40 cycles of 95°C for 20 s and 60°C for 30 s. The reaction for each sample was performed in triplicate. The expression level of *ß-actin* was used for normalization. A cycle threshold of 38 was designated arbitrarily as 1.

Ad293 and MIN6 cells lentiviral transduction

Lentiviral vector construction and viral particle packaging were performed by GeneCopoeia (Guangzhou, China). To generate Ad293CreER cells, Ad293 cells were infected with lentiviral particles (multiplicity of infection [MOI] = 10) carrying a *CMV-CreER* expression cassette (*Lenti-CMV-CreER*) in the presence of 5 μg/mL Polybrene (Sigma-Aldrich, St. Louis, MO). Cells were collected at 24 h after infection, and a single cell was seeded in 96-well. Ad293CreER clones were generated after approximately 7 days of cultivation, verified by transfection with the Cre-reporter. To examine the labeling specificity and tightness of CreER or mCreER under the control of the RIP promoter, Ad293 cells and MIN6 cells (generously provided by Dr. Cai of the National Institutes of Health and have been examined routinely to be mycoplasma free), cells were infected by either *Lenti-RIP-CreER* or *Lenti-RIP-mCreER/Lenti-CMV-mTEVp* (MOI = 10) in the presence of 5 μg/mL polybrene. Cells were simultaneously transfected with the Cre reporter and imaged at 24 h and 48 h after induction using a fluorescence microscope equipped with a CCD camera (Nikon, Eclipse TE 2000).

Measurement of insulin secretion and insulin content

MIN6 cells seeded overnight in 96-wells were infected with *Lenti-RIP-CreER*, or *Lenti-RIP-mCreER/Lenti-CMV-mTEVp* or control lentiviral particles *Lenti-CMV-EGFP*. MIN6 cells 48 h after infection were used for the insulin secretion assay as described previously.[54] Cells were washed twice with 100 μL glucose-free KRB followed by preincubation for 1 h at 37°C in 100 μL glucose-free KRB. Next, cells were washed twice with glucose free KRB prior to a 1-h incubation in 100 μL KRB including 2.5 mM or 25 mM glucose at 37°C. At the end of the incubation, cell debris-free supernatants were used for insulin measurement with a Rat/Mouse Insulin ELISA Kit (EMD Millipore Corporation, Darmstadt, Germany) according to the protocol provided by the company. To normalize the amount of secreted insulin, cells in each well were lysed with RIPA buffer (Beyotime, Shanghai, China), and protein concentration of the lysates was measured using the BCA protein assay kit (Beyotime, Shanghai, China). The insulin secretion was expressed as the amount of insulin (in nanograms) per milligram protein. At the end of the incubation MIN6 cells for insulin content measurement. To this end, 100 μL of acidified ethanol (0.15 M HCl in 75% ethanol in H_2O) were added to 96-wells. Insulin was extracted at 4°C for 16 h. The supernatants were collected, and insulin content was determined using a rat/mouse insulin ELISA Kit. The results were normalized to the protein concentration of the lysates.

Statistics

All experiments were assayed at least three times. All statistical analyses were performed using GraphPad Prism 7.0 (GraphPad Software, San Diego, CA). Data are presented as a mean ± standard error of the mean. The results were subjected to unpaired Student's *t* test, one-way ANOVA with Sidak's multiple comparison test, or two-way ANOVA

with a Bonferroni adjustment for multiple comparisons. A p value of less than .05 was considered statistically significant.

SUPPLEMENTAL INFORMATION

Supplemental information can be found online at https://doi.org/10.1016/j.omtn.2022.01.022.

ACKNOWLEDGMENTS

Supported by the Natural Science Foundation of Guangdong (http://gdstc.gd.gov.cn/ Grant No. 2019A1515011547); Science and technology bureau of Shantou City (Grant No. 2016-30); Guangdong High-Level University Project "Green Technologies for Marine Industries"; and Li Ka Shing Foundation (Grant No. 2020LKSFG10C). Informed consent was obtained from all individual participants included in the study.

AUTHOR CONTRIBUTIONS

M.C., X.T., L.X., R.W., and H.H. conducted the experiments. H.Z. and W.X. designed the experiment. M.C. and C.W. wrote the paper. All authors had approved the final version of the article. C.W. takes full responsibility for the content of the article.

DECLARATION OF INTEREST

No competing financial interests exist.

REFERENCES

1. Kretzschmar, K., and Watt, F.M. (2012). Lineage tracing. Cell *148*, 33–45.
2. Baron, C.S., and Oudenaarden, A.V. (2019). Unravelling cellular relationships during development and regeneration using genetic lineage tracing. Nat. Rev. Mol. Cell Biol. *20*, 753–765.
3. Kebschull, J.M., and Zador, A.M. (2018). Cellular barcoding: lineage tracing, screening and beyond. Nat. Methods *15*, 871–879.
4. VanHorn, S., and Morris, S.A. (2021). Next-generation lineage tracing and fate mapping to interrogate development. Dev. Cell *56*, 7–21.
5. Feil, R., Wagner, J., Metzger, D., and Chambon, P. (1977). Regulation of Cre recombinase activity by mutated estrogen receptor ligand-binding domains. Biochem. Biophys. Res. Commun. *237*, 752–757.
6. Sauer, B. (1987). Functional expression of the cre-lox site-specific recombination system in the yeast Saccharomyces cerevisiae. Mol. Cell Biol. *7*, 2087–2096.
7. Sauer, B., and Henderson, N. (1988). Site-specific DNA recombination in mammalian cells by the Cre recombinase of bacteriophage P1. Proc. Natl. Acad. Sci. U.S.A *85*, 5166–5170.
8. Gu, H., Marth, J.D., Orban, P.C., Mossmann, H., and Rajewsky, K. (1994). Deletion of a DNA polymerase beta gene segment in T cells using cell type-specific gene targeting. Science *265*, 103–106.
9. Tsien, J.Z., Huerta, P.T., and Tonegawa, S. (1996). The essential role of hippocampal CA1 NMDA receptor-dependent synaptic plasticity in spatial memory. Cell *87*, 1327–1338.
10. Phillip, A.D., Nayak, S., Corti, M., Morel, L., Herzog, R.W., and Byrne, B.J. (2016). Targeted approaches to induce immune tolerance for Pompe disease therapy. Mol. Ther. Methods Clin. Dev. *27*, 15053.
11. Alvarez-Aznar, A., Martinez-Corral, I., Daubel, N., Betsholtz, C., Makinen, T., and Gaengel, K. (2019). Tamoxifen-independent recombination of reporter genes limits lineage tracing and mosaic analysis using CreERT2 lines. Transgenic Res. *29*, 1–16.
12. Sebastian, S.A., and Greter, M. (2020). STOP floxing around: specificity and leakiness of inducible Cre/loxP systems. Eur. J. Immunol. *50*, 338–341.
13. Richard, K., Heather, I., Elizabeth, C., Carol, H., Louise, H., and Winton, D.J. (2004). Elimination of background recombination: somatic induction of Cre by combined transcriptional regulation and hormone binding affinity. Nucleic Acids Res. *32*, e92.
14. Kristianto, J., Johnson, M.G., Zastrow, R.K., Radcliff, A.B., and Blank, R.D. (2017). Spontaneous recombinase activity of Cre-ERT2 *in vivo*. Transgenic Res. *26*, 411–417.
15. Ji-Yeon, L., Ristow, M., Lin, X.Y., White, M.F., Magnuson, M.A., and Hennighausen, L. (2006). RIP-Cre revisited, evidence for impairments of pancreatic beta-cell function. J. Biol. Chem. *3*, 2649–2653.
16. Semprini, S., Troup, T.J., Kotelevtseva, N., King, K., Davis, J.R., Mullins, L.J., Chapman, K.E., Dunbar, D.R., and Mullins, J.J. (2007). Cryptic loxP sites in mammalian genomes: genome-wide distribution and relevance for the efficiency of BAC/PAC recombineering techniques. Nucleic Acids Res. *35*, 1402–1410.
17. Liu, Y., Suckale, J., Masjkur, J., Magro, M.G., Steffen, A., Anastassiadis, K., and Solimena, M. (2010). Tamoxifen-independent recombination in the RIP-CreER mouse. PLoS One *5*, e13533.
18. Shiota, C., Prasadan, K., Guo, P., Fusco, J., and Xiao, X.W. (2017). Gcg CreERT2 knockin mice as a tool for genetic manipulation in pancreatic alpha cells. Diabetologia *60*, 2399–2408.
19. Lesaffer, B., Verboven, E., Huffel, L.V., Moya, I.M., Grunsven, L.V., Leclercq, I.A., Lemaigre, F.P., and Halder, G. (2019). Comparison of the Opn-CreER and Ck19-CreER drivers in bile ducts of normal and injured mouse livers. Cells *8*, E380.
20. Seime, T., Kolind, M., Mikulec, K., Mikulec, K., Summers, M.A., Cantrill, L., Little, D.G., and Schindeler, A. (2015). Inducible cell labeling and lineage tracking during fracture repair. Dev. Growth Differ. *57*, 10–23.
21. Dor, Y., Brown, J., Martinez, O.I., and Melton, D.A. (2004). Adult pancreatic beta-cells are formed by self-duplication rather than stem-cell differentiation. Nature *429*, 41–46.
22. Nir, T., Melton, D.A., and Dor, Y. (2007). Recovery from diabetes in mice by β cell regeneration. J. Clin. Invest. *117*, 2553–2561.
23. Teta, M., Rankin, M.M., Long, S.Y., Stein, G.M., and Kushner, J.A. (2007). Growth and regeneration of adult β cells does not involve specialized progenitors. Dev. Cell *12*, 817–826.
24. Ku, H.T. (2008). Minireview: pancreatic progenitor cells–recent studies. Endocrinology *149*, 4312–4316.
25. Domínguez-Bendala, J., Qadir, M.M.F., and Pastori, R.L. (2019). Pancreatic progenitors: there and back again. Trends Endocrinol. Metab. *30*, 4–11.
26. Inada, A., Nienaber, C., Katsuta, H., Fujitani, Y., Levine, J., Morita, R., Sharma, A., and Bonner-Weir, S. (2008). Carbonic anhydrase II-positive pancreatic cells are progenitors for both endocrine and exocrine pancreas after birth. Proc. Natl. Acad. Sci. U.S.A *105*, 19915–19919.
27. Wang, D.S., Wang, J.Q., Bai, L.Y., Pan, H., Feng, H., Clevers, H., and Zeng, Y.A. (2020). Long-term expansion of pancreatic islet organoids from resident $Procr^{+}$ progenitors. Cell *180*, 1198–1211.
28. Li, Y., He, L.J., Huang, X.Z., Bhaloo, S.I., Zhao, H., Zhang, S.H., Pu, W.J., Tian, X.Y., Li, Y., Lui, Q.Z., et al. (2018). Genetic lineage tracing of nonmyocyte population by dual recombinases. Circulation *138*, 793–805.
29. Medema, J.P. (2013). Cancer stem cells: the challenges ahead. Nat. Cell Biol. *15*, 338–344.
30. Lexow, J., Poggioli, T., Sarathchandra, P., Santini, M.P., and Rosenthal, N. (2013). Cardiac fibrosis in mice expressing an inducible myocardial-specific Cre driver. Dis. Model. Mech. *6*, 1470–1476.
31. Bersell, K., Choudhury, S., Mollova, M., Polizzotti, B.D., and Ganapathy, B. (2013). Moderate and high amounts of tamoxifen in αMHC-MerCreMer mice induce a DNA damage response, leading to heart failure and death. Dis. Model. Mech. *6*, 1459–1469.
32. Higashi, A.Y., Ikawa, T., Muramatsu, M., Economides, A.N., Niwa, A., Okuda, T., Murphy, A.J., Rojas, J., Heike, T., and Nakahata, T. (2009). Direct hematological toxicity and illegitimate caused by the systemic activation of CreERT2. J. Immunol. *182*, 5633–5640.
33. Kang, J., Ferguson, D., Song, H., Bassing, C., Eckersdorff, M., Alt, F.W., and Xu, Y. (2005). Functional interaction of H2AX, NBS1, and p53 in ATM-dependent DNA damage responses and tumor suppression. Mol. Cell Biol. *25*, 661–670.

34. Lexow, J., Poggioli, T., Sarathchandra, P., Santini, M.P., and Rosenthal, N. (2015). Phenotypic characterization of MIP-CreERT1Lphi mice with transgene-driven islet expression of human growth hormone. Diabetes *64*, 3798–3807.

35. Gong, G.C., Fan, W.Z., Li, D.Z., Tian, X., Chen, S.J., Fu, Y.C., Xu, W.C., and Wei, C.J. (2015). Increased specific labeling of INS-1 pancreatic beta-cell by using RIP-driven Cre mutants with reduced activity. PLoS One *10*, e0129092.

36. Jullien, N., Sampieri, F., Enjalbert, A., and Herman, J.P. (2003). Regulation of Cre recombinase by ligand-induced complementation of inactive fragments. Nucl. Acids Res. *31*, e131.

37. Weinberg, B.H., Cho, J.H., Agarwal, Y., Pham, N.T., Caraballo, L.D., Walkosz, M., Ortega, C., Trexler, M., Tague, T., Law, B., et al. (2019). High-performance chemical- and light-inducible recombinases in mammalian cells and mice. Nat. Commun. *10*, 4845.

38. Wu, J., Wang, M., Yang, X., Yi, C., and Ye, H. (2020). A non-invasive far-red light-induced split-Cre recombinase system for controllable genome engineering in mice. Nat. Commun. *11*, 3708.

39. Zhang, Y., Riesterer, C., Ayrall, A.M., Sablitzky, F., Littlewood, T.D., and Reth, M. (2003). Inducible site-directed recombination in mouse embryonic stem cells. Nucleic Acids Res. *24*, 543–**54**8.

40. Matsuda, T., and Cepko, C.L. (2007). Controlled expression of transgenes introduced by *in vivo* electroporation. Proc. Natl. Acad. Sci. USA ***104***, 1027–1032.

41. Kam, M.K., Lee, K.Y., Tam, P.K., and Lui, V.C. (2012). Generation of NSE-MerCreMer transgenic mice with tamoxifen inducible Cre activity in neurons. PLoS One *7*, e35799.

42. Jones, T.I., Chew, G.L., Barraza-Flores, P., Schreier, S., Ramirez, M., Wuebbles, R.D., Burkin, D.J., Bradley, R.K., and Jones, P.L. (2020). Transgenic mice expressing tunable levels of DUX_4 develop characteristic facioscapulohumeral muscular dystrophy - like pathophysiology ranging in severity. Skelet. Muscle *10*, 8.

43. Aumais, J.P., Lee, H.S., Lin, R., and White, J.H. (1997). Selective interaction of hsp90 with an estrogen receptor ligand-binding domain containing a point mutation. J. Biol. Chem. *272*, 12229–12235.

44. Zhong, W., and Reinherz, E.L. (2005). CD8 alpha alpha homodimer expression and role in CD8 T cell memory generation during influenza virus A infection in mice. Eur. J. Immunol. *35*, 3103–3110.

45. Harder, B., Schomburg, A., Pflanz, R., Küstner, K., Gerlach, N., and Schuh, R. (2008). TEVprotease-mediated cleavage in Drosophila as a tool to analyze protein functions in living organisms. Biotechniques *44*, 765–772.

46. Cesaratto, F., Burrone, O.R., and Petris, G.J. (2016). Tobacco Etch Virus protease: a shortcut across biotechnologies. J. Biotechnol. *231*, **23**9–249.

47. Wang, Z.V., Mu, J., Schraw, T.D., Gautron, L., Elmquist, J.K., Zhang, B.B., Brownlee, M., and Scherer, P.E. (2008). PANIC-ATTAC: a mouse model for inducible and reversible beta-cell ablation. Diabetes *57*, 2137–2148.

48. Burnett, S.H., Kershen, E.J., Zhang, J.Y., Zeng, L., Straley, S.C., Kaplan, A.M., and Cohen, D.A. (2004). Conditional macrophage ablation in transgenic mice expressing a Fas-based suicide gene. J. Leukoc. Biol. *75*, 612–623.

49. Mabe, S., Nagamune, T., and Kawahara, M. (2014). Detecting protein-protein interactions based on kinase-mediated growth induction of mammalian cells. Sci. Rep. *1*, 61**2**7.

50. Clackson, T., Yang, W., Rozamus, L.W., Hatada, M., Amara, J.F., Rollins, C.T., Stevenson, L.F., Magari, S.R., Wood, S.A., Courage, N.L., et al. (1998). Redesigning an FKBP-ligand interface to generate chemical dimerizers with novel specificity. Proc. Natl. Acad. Sci. U.S.A *95*, **10**437–10442.

51. Madugula, V., and Lu, L. (2016). A ternary complex comprising transportin1, Rab8 and the ciliary targeting signal directs proteins to ciliary membranes. J. Cell Sci. *129*, 3922–3934.

52. Daringer, N.M., Dudek, R.M., Schwarz, K.A., and Leonard, J.N. (2014). Modular extracellular sensor architecture for engineering mammalian cell-based devices. ACS Synth. Biol. *12*, 892–902.

53. Eguchi, T., Sogawa, C., Matsumoto, M., Tran, M.T., Okusha, Y., Lang, B.J., Okamoto, K., and Calderwood, S.K. (2020). Cell stress induced stressome release including damaged membrane vesicles and extracellular HSP90 by prostate cancer cell. Cells *9*, 755.

54. Wang, N., Guo, D.Y., Tian, X., Lin, H.P., Li, Y.P., Chen, S.J., Fu, Y.C., Xu, W.C., and Wei, C.J. (2016). Niacin receptor GPR109A inhibits insulin secretion and is down-regulated in T2DM islet beta-cells. Gen. Comp. Endocrinol. *237*, 98–108.